FULL PAPER

Self-assembled Cofacial Zinc Porphyrin Supramolecular Nanocapsules as tuneable $^1O_2$ Photosensitizers

Cédric Colomban[a], Carles Fuertes-Espinosa[a], Sébastien Goeb[b], Marc Sallé[b], Miquel Costas[a], Lluis Blancafort*[a] and Xavi Ribas*[a]

Abstract: Here we demonstrate the benefits of using cofacial Zn-porphyrins, used as structural synthons in coordination-driven self-assembled prisms, to produce cage-like singlet oxygen photosensitizers having tuneable photosensitizing properties. In particular, we describe the photosensitizing and emission properties of palladium and copper-based supramolecular capsules **1** and **2** and demonstrate that the nature of the bridging metal nodes in these discrete self-assembled prisms strongly influence the $^1O_2$ generation at the Zn-porphyrin centers. On one hand, the Pd(II)-based prism **1** was found to be a particularly robust photosensitizer, while on the other hand the Cu^{II} self-assembly **2** is a dormant photosensitizer that can be switched to a ON state upon disassembly of the supra-structure. Furthermore, the well-defined cavity within **1** and **2** allow for the encapsulation of pyridine-based ligands and fullerene derivatives, leading to a remarkable guest tuning of the $^1O_2$ production.

Introduction

Singlet oxygen ($^1O_2$), the lowest excited state of oxygen plays an important role in many biological oxidative processes (e.g. natural biological defence processes and cytotoxic agent in phototherapies).[1] This reactive oxygen species (ROS) is not only highly desired because of its applications in photodynamic cancer therapy (PDT) but is also a very convenient oxidant for wastewater treatments or organic photoredox reactions.[2,3,4] Porphyrin derivatives are currently the most used $^1O_2$ photosensitizers due to their high quantum yield in $^1O_2$ generation and high light-absorption capability.[5] The construction of optimized $^1O_2$ photosensitizers with high efficiency, stability and control over $^1O_2$ production is a topic of intensive research and many efforts have been devoted recently in this direction. For example, the suppression of self-quenching of the excited state, observed upon formation of porphyrin aggregates, could be prevented by decorating a porphyrin derivative with bulky noncovalent building blocks.[6] To enhance the $^1O_2$ productivity, another strategy consists in using phthalocyanine[5] or porphyrin-based [7] conjugated microporous polymers. Furthermore, porphyrinic-based metal-organic frameworks (MOFs) have been reported as efficient tools for reversible control over the $^1O_2$ generation[8] or selective photo-oxidation.[9] In light of these recent examples, controlling the second coordination sphere of porphyrinic derivatives appears as a powerful strategy for the development of innovative photosensitizers.

On the other hand, porphyrin based supramolecular cages have recently attracted lots of attention. The self-assembly of molecular barrels with porphyrin walls,[10] coordination prisms with porphyrin faces, [11] supramolecular arrays of one porphyrin and one phthalocyanine linked by rotaxane nodes, [12] and even multiporphyrin cages,[13] have been successfully described using different bridging metals (Pd, Pt, Zn). The usefulness of porphyrin-based capsules for versatile applications ranging from binding and separation of fullerenes, [14] spin crossover, [15] cooperative binding of anionic and neutral guest species, [16] to water solubilisation of hydrophobic cargo, [17] and preparation of breathing flexible cages, [18] have been recently established. Furthermore, the well-defined cavity found in these systems has also been used as a scaffold for the isolation of metallo-catalysts aiming at performing catalysis in confined space.[19,20,21] Porphyrin and Zn-porphyrin moieties are commonly considered as inert building blocks in these supramolecular architectures and few precautions are usually taken regarding their exposure to natural light. However, porphyrins and metalloporphyrins are well-known photosensitizers and the production of reactive $^1O_2$ might impact the way that both host-guest chemistry and catalysis proceeds within theses cargos. Very few examples of self-assembled nanocages used as homogeneous photosensitizers are described in the literature. Ruthenium-based self-assembled porphyrin prisms were studied as phototoxic agents by Therrien and co-workers.[22] They reported octanuclear ruthenium arene metalla-cubes composed of cofacial tetrapyridyl porphyrin panels, as chemotherapeutics in cancer cells.[23] In any case, the effect of the prismatic structure toward the stability, emission and photosensitizing properties of the porphyrin center were not investigated.

Herein we present a novel approach to build photosensitizers integrating the principles of self-assembly, host-guest chemistry and photochemistry. We report the study of the singlet oxygen photosensitization efficiency of two self-assembled metal-organic capsules. In order to vary the nature of the metal-nodes we studied the self-assembled tetragonal prismatic compounds **1** and **2**, where two cofacial Zn-porphyrins are bound by four

[a] Dr. C. Colomban, C.Fuertes-Espinosa, Dr. M. Costas, Dr. L. Blancafort, Dr. X. Ribas.
Institut de Química Computatcional i Catàlisi (IQCC) and Departament de Química, Universitat de Girona,
Campus Montilivi, Girona, E17003, Catalonia, Spain
E-mail: xavi.ribas@udg.edu ; lluis.blancafort@udg.edu

[b] Dr. S. Goeb, Prof. M. Sallé
Université d'Angers, CNRS UMR 6200
Laboratoire MOLTECH-Anjou
2 bd Lavoisier, 49045 Angers Cedex (France)

Supporting information for this article is given via a link at the end of the document.

bridging macrocyclic walls respectively interconnected by Pd^{II} or Cu^{II}–carboxylate bonds (Figure 1). We discovered that the nature of the metal nodes in the supramolecular structures determines their ability to produce $^1O_2$. More remarkably, guest binding can also modify the $^1O_2$ production efficiency. This work is of fundamental nature and aims at giving a proof of concept for the potential benefits of the development of self-assembled Zn-porphyrin supramolecular capsules as $^1O_2$ photosensitizers or dormant-photosensitizer under supramolecular control.

Results and Discussion.

Palladium-based prism 1 as $^1O_2$ sensitizer

The redox-controlled encapsulation of an extended tetrathiafulvalene-based switchable guest, **(m-Py)exTTF** in the cavity of **1** has been recently described.[24] On the other hand extended (exTTF) [25] and superextended (sExTTF) tetrathiafulvalene[26] derivatives are able to rapidly quench $^1O_2$ produced by a photosensitizer, by degradation into corresponding quinone products, making them interesting $^1O_2$ sensors. On this basis, we envisioned that the encapsulated ligand in the **(*m*-Py)exTTF⊂1** supra-structure (Figure 1a) might react with the putative $^1O_2$ produced at the Zn-porphyrin centers of **1**.

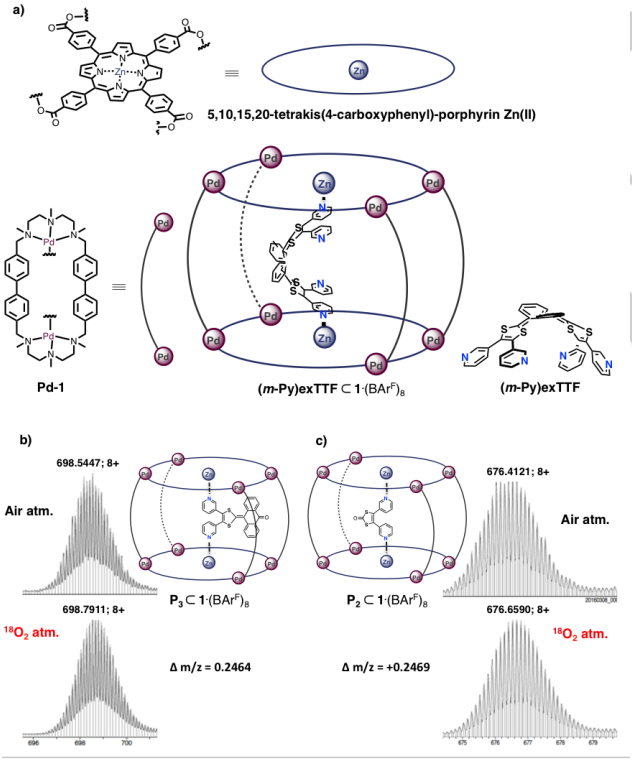

Figure 1. (a) Schematic representation of the building blocks used for the synthesis of the nanocapsule **1** together with the envisioned structure of **(*m*-Py)exTTF⊂1**. (b) Schematic representation of the envisioned structure of the **P₃⊂1** host-guest adduct with the respective ESI-HRMS spectra obtained under air or ^{18}O-labeled O_2 atmosphere. (c) idem for **P₂⊂1**.

Indeed, while the encapsulation of **(m-Py)exTTF** by **1** in dark conditions leads to the formation of the **(*m*-Py)exTTF⊂1** complex in a 1:1 stoichiometry,[24] its exposure to natural light under aerobic atmosphere (during 5 and 90 min) yields to the progressive formation of the keto products **P₂** and **P₃** arising from the photo-oxidation of the C=C bond of **(*m*-Py)exTTF**. Interestingly, both products were detected by ESI-HRMS as host-guest adducts **P₂⊂1** and **P₃⊂1** (Figure 1b-c, Figure S1-S5). Upon longer exposition time (270 min) **P₂⊂1** was present as the major species, while only trace amount of **P₃⊂1** was detected (Figure S6, S7). These observations strongly suggest that **P₃** generated during the early stage of the reaction is further oxidized into **P₂**. Natural light and air exposure of the authentic sample of **P₃⊂1**, prepared independently, confirms this proposal (Figure S8). It is worth noting that cage **1**, natural light, and dioxygen were all necessary for this reaction to take place. In the absence of any of these components, either none or only traces of the oxidation products **P₂** and **P₃** were detected (Figure S9, S10). Furthermore, performing the reactions in the presence of $^{18}O_2$ lead to the incorporation of $^{18}O_2$ in the oxidized products **^{18}O-P₂** and **^{18}O-P₃** (Figure 1 and S11). Finally, when reactions were conducted in the presence of $H_2{}^{18}O$ under a $^{16}O_2$ atmosphere, no ^{18}O was incorporated into products (Figure S12), discarding the hypothesis of a reaction involving a photo-induced π radical cation species **(m-Py)exTTF$^{\bullet+}$** which is subsequently trapped by O_2 or H_2O.[27] Altogether, these results strongly suggest that the oxidizing species is coming from an activation of molecular oxygen $^3O_2$ into the reactive $^1O_2$. Oxidation of **(*m*-Py)exTTF** under natural light and air, in CH_3CN / CH_2Cl_2 1:9, in presence of a catalytic amount of **1** (1.0 mol %) was followed by ^1H NMR. Interestingly, upon 16 h of light exposure, a 65% conversion of the substrate, to yield **P₃**, **P₂** and anthraquinone (**AQ**) products, was observed (Figure 2). By increasing the catalyst loading to 4.0 mol% a complete conversion of **(*m*-Py)exTTF** into **P₂** and **AQ** was reached after 3 hours of light exposure indicating a continuous production of $^1O_2$ by **1**.[28]

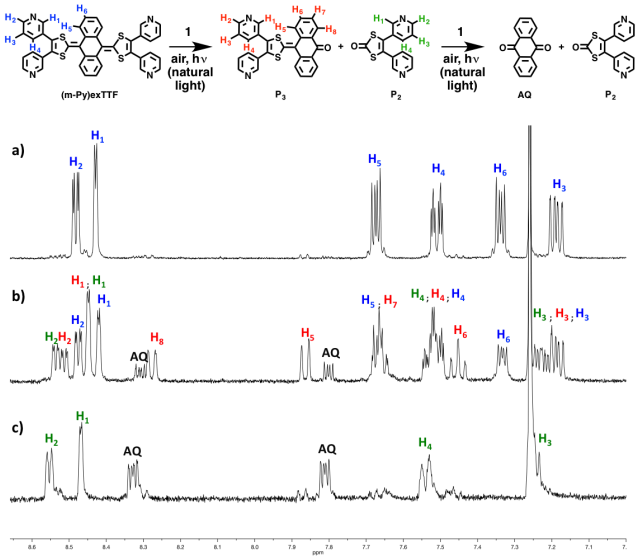

Figure 2. ^{1}H NMR monitoring of the photocatalytic oxidative cleavage of ***(m*-Py)exTTF**, a) in the absence of light, no degradation was observed, b) in the presence of **1** (1.0 mol%) after 16h of light exposure and c) in the presence of **1** (4.0 mol%) after 3 hours of light exposure.

The ability of cage **1** to generate singlet oxygen was then monitored upon irradiation with a 575 nm lamp by using 9,10-diphenylanthracene (DPA) as $^{1}O_2$ quencher. In the presence of catalytic amounts of **1** (1.3 mol%), a decay in absorbance occurs at 340, 356, 375 and 393 nm (corresponding to the absorption bands of DPA, Figure 3a) as a consequence of the formation of the corresponding endoperoxide which does not absorb, (Figure 3b) confirming the generation of $^{1}O_2$.[29]

As a control experiment, DPA (0.1 x 10^{-3} M) alone was irradiated under air in CH_2Cl_2/CH_3CN 9:1. A limited decrease in the absorbance of DPA was observed, revealing its stability under the experimental conditions (Figure S14).[30] On the other hand, zinc−tetraphenylporphyrin (**ZnTPP**), is a widely used photosensitizer which displays high quantum yield toward $^{1}O_2$ generation, good solubility in organic solvent, and a well-studied photochemistry.[31] **ZnTPP** was therefore chosen as reference photosensitizer in the present study. Reactions carried out with the same catalyst loading (1.3 mol%) of **1** and **ZnTPP** displayed identical DPA decay, revealing similar efficiency in $^{1}O_2$ generation per molecular system (Figure 3c). However it should be noted that the $^{1}O_2$ production rate per Zn-porphyrin center is for **1** is half the one observed for monomeric **ZnTPP**.[32] According to the accepted mechanism, $^{1}O_2$ is generated by energy transfer from the T_1 state of the photosensitizer to $^{3}O_2$. The calculated triplet energies for **1** and **ZnTPP**, are respectively 1.65 and 1.63 eV (Table 1 and S1, see ESI for computation details). These roughly similar triplet energies are in line with the similar activities towards $^{1}O_2$ generation observed for the single molecular photosensitizers **1** and **ZnTPP**. For comparison, the experimental triplet energy of **ZnTPP** is 1.59 eV,[33] in good agreement with the calculation.

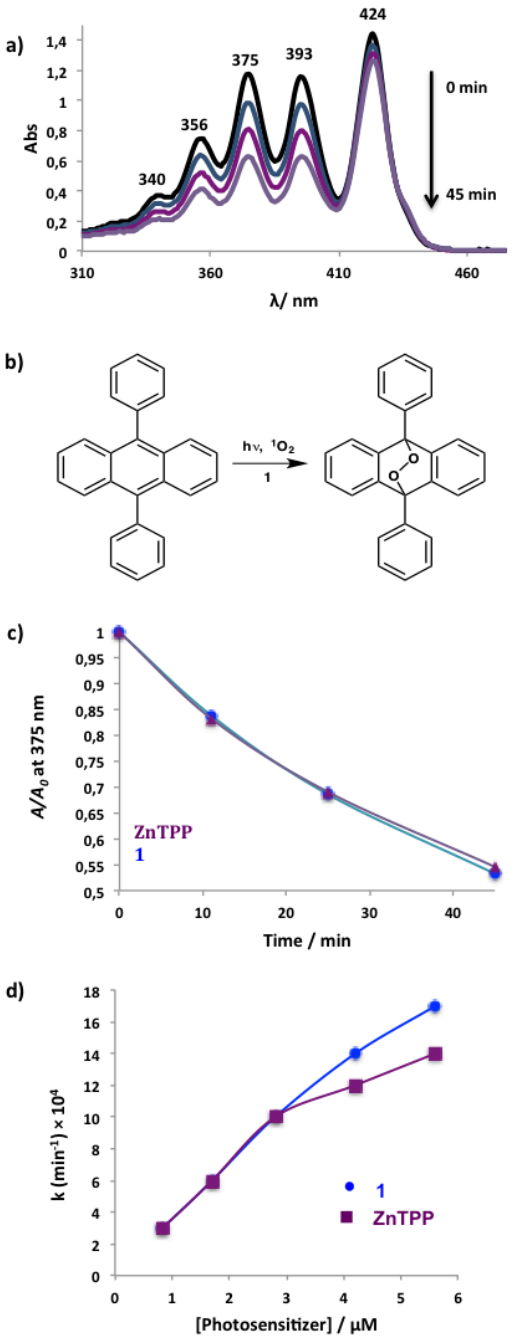

Figure 3. a) Time-dependent absorption spectra of DPA (0,1 x 10^{-3} M) in CH_2Cl_2/CH_3CN (9:1) under air, upon irradiation at 575 nm in the presence of **1** (1.3 mol%); the band at 424 nm corresponds to the Soret of **1,** b) Reaction of 9,10-diphenylanthracene (DPA) with $^{1}O_2$ yielding its corresponding endoperoxide and c) comparison of the decay rate of DPA in the presence of **1** (1.3 mol%, blue circle) or **ZnTPP** (1.3 mol%, purple triangle). d) Kinetics of the photooxidation of DPA in CH_2Cl_2/CH_3CN 9:1. k_{obs} *vs.* concentration of **1** (blue circles) and **ZnTPP** (purple squares)

Kinetic experiments were performed by monitoring the bleaching of the absorption band of DPA in CH_2Cl_2/CH_3CN 9:1 as a function of the irradiation time and at several concentrations of **1** and **ZnTPP**. The resulting kinetic profiles were linear over time for both photosensitizers, attesting for a zero-order dependence on [DPA], typical of the photooxidation of DPA by $^1O_2$ (Figure S15 and S16).[34] Observed constants k_{obs} were extracted from these data. Interestingly for the oxidation of DPA sentitized by increasing amounts of **1** the k_{obs} increase linearly in the concentration range 0,84 - 5.6 x 10^{-6} M. In the case of **ZnTPP** the k_{obs} value response does not increase linearly, but instead two different linear regimes are observed. From [**ZnTPP**] = 0.84 x 10^{-6} M to 3 x 10^{-6} M, the increase and k_{obs} values overlay with those obtained with **1**. However, a slower increase is observed at high concentration (3.0 – 5.6 x 10^{-6} M, Figure 3d). Similar trends are observed by ploting the k_{obs} values versus the concentration of Zn-porphyrin center for both photosensitizers (Figure S17). The concentration dependent deactivation of the $^1O_2$ production observed in the case of **ZnTPP** might be explained by a difference in the stability toward photobleaching, which is more pronounced at higher concentrations of the photosensitizer.

Stability towards photobleaching

Despite their wide use as photosensitizer, the photostability of metallo-porphyrins is strongly limited by their reaction with $^1O_2$, resulting in a self-destruction by photo-oxygenation.[35] Therefore, stability toward $^1O_2$ attack and intrinsic light stability, are highly desirable properties. The bleaching of **ZnTPP** and **1** (1.7 x 10^{-6} M) were compared by following the decay of their Soret bands by UV-vis, upon irradiation at 575 nm, under air in CH_2Cl_2/CH_3CN (9:1) (Figure 4). Interestingly, the decay rate of cage **1** is much slower than the reference **ZnTTP**. After 8 h of irradiation, 91% of the initial Soret band intensity degrades in the case of **ZnTPP**, whereas only a 24% decrease is observed for **1** (Figure 4c). Furthermore, It should be noted that a similar trend was observed by comparing the bleaching of **1** and the tetracarboxyphenyl zinc porphyrin (**Zn-TCPP),** indicating that the enhanced resistance of **1** should be attributed to the nanocapsule stability and not solely to the carboxylate substituents (Figure S18).

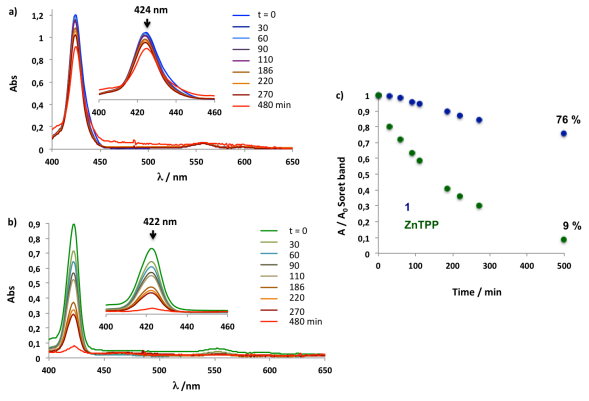

Figure 4. Time-dependent absorption spectra of (a) **1** and (b) **ZnTPP** (1.7 x 10^{-6} M), in CH_2Cl_2/CH_3CN (9:1) under air upon irradiation at 575 nm, c) corresponding decay rate of Soret bands of **1** (blue) and **ZnTPP** (green).

Since **1** and **ZnTPP** (1.7 x 10^{-6} M) display similar photosensitization activities (Figure 3), their respective stability cannot be explained by the amount of $^1O_2$ produced over the experiment time. According to the literature, the attack of $^1O_2$ at the *meso*-position of the porphyrin is a major degradation pathway.[36] It has been reported that porphyrin can be protected from attack by $^1O_2$ by sterically shielding the *meso*-positions of the porphyrin ring with blocking substituents (fluorine, chlorine, methoxy groups) on the 2- and 6- positions of the aryl rings groups.[31,37] Furthermore, It has already been demonstrated that the presence of appropriate electron-withdrawing substituents on tetraphenyl-based porphyrin macrocycles can limit their photo-oxygenation at the *meso* position.[38] The remarkable stability of **1** toward bleaching can be therefore explained by the conjunction of two factors: *a)* the sterical hindrance arising from the supramolecular coordination of the Pd-macrocyclic wall at the *meso*-position of the Zn-porphyrin units and *b)* the electronic effects due to the presence of four coordination bonds (Pd-carboxylate) in each porphyrin, which strongly decrease their electron density. A comparison of the electrochemical behavior of **1** and **ZnTPP** confirms that the first porphyrin oxidation is shifted to higher potential (ΔE= +186 mV) in the case of the supramolecular cage **1** (Figure S19, S20).

The photocatalytic robustness of **1** and **ZnTPP** were then investigated toward the simple C=C bond cleavage of $\mathbf{P_3}$ (into $\mathbf{P_2}$ and **AQ**) through recycling experiments.[39] A solution of $\mathbf{P_3}$ (4.2 x 10^{-5} M; 8.4 x 10^{-8} mol) in CH_2Cl_2 / CH_3CN 9:1 was irradiated for 45 min in the presence of catalytic amount (4.0 mol%) of photosensitizers **1** or **ZnTPP**. After this irradiation time, fresh $\mathbf{P_3}$ substrate was added to each solution in order to reach the initial quantity of $\mathbf{P_3}$. The procedure was repeated to obtain five catalytic cycles (Figure 5). Interestingly, **ZnTPP** showed a strong deactivation after the first recycle run (from 38 % to 6.5% conversion), while **1** displayed a much more robust behaviour with respectively 46, 39, 31, 20 and 8.5 % conversion upon five catalytic cycles.

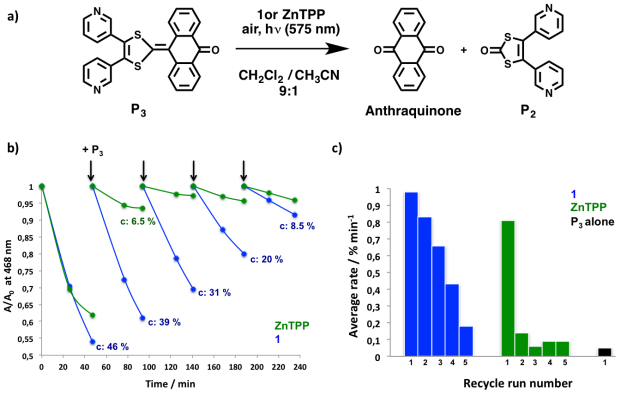

Figure 5. (a) Reaction of $\mathbf{P_3}$ with $^1O_2$ yielding to the formation of $\mathbf{P_2}$ and anthraquinone, (b) comparison of the decay rate of $\mathbf{P_3}$ in the presence of **ZnTPP** (4.0 mol%; green) or **1** (4.0 mol%; blue) upon successive additions of substrate (arrows represents adjusted additions of $\mathbf{P_3}$ to recover the initial amount of substrate; **c** represents the P_3 conversion) and (c) comparison of the average

decay rate of **P₃** within a 45 min irradiation time, upon recycling experiments, using **1** (blue), **ZnTPP** (green).

Guest-dependent tuning of $^1O_2$ production.

Taking advantage of the well-defined cavity present in prism **1**, we investigated the $^1O_2$ production efficiency upon guest encapsulation. Pyridine-based ligands like **4,4'-bipy** and **(*m*-Py)exTTF** are strongly accommodated within the cavity of **1** via the ability of the Zn-porphyrin to interact with their pyridine moieties.[20,24] Time-dependent plots of the absorbance of DPA in presence and absence of **4,4'-bipy** reveal a higher consumption (by a factor 1.4) when the host-guest adduct **4,4'-bipy⊂1** was used as photosensitizer (Figure 6) with a conversion of 40% after 20 min while only 28% conversion were observed for **1**.

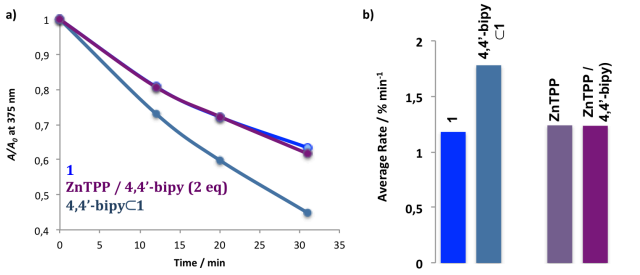

Figure 6. (a) Comparison of the decay rate of DPA in CH_2Cl_2/CH_3CN (9:1) under air upon irradiation at 575 nm (0.1 x 10^{-3} M), in the presence of **1** (1.3 mol%; blue), **4,4-bipy⊂1** (1.3 mol%; pale blue) and **ZnTPP** (1.3 mol%) together with 4,4-bipy (2.6 mol%; purple) (b) Comparison of the average decay rate of DPA within a 45 min irradiation time, using **1** (blue) or **ZnTPP** (purple) as photosensitizers with or without additions of **4,4-bipy** (2 equiv.) to the reaction mixture.

Similar experiments were carried out with **(*m*-Py)exTTF⊂1** and **P₃⊂1** (Figure S23). Both host-guest systems exhibit identical results to those obtained with **4,4'-bipy⊂1** (Figure S24), suggesting similar rates of $^1O_2$ generation. Therefore, the axial binding of a pyridine moiety to each of the Zn-porphyrin centers of **1** plays an essential role in the observed increase of $^1O_2$ production. As expected, the ditopic binding of **4,4'-bipy** within **1** in CH_2Cl_2 leads to bathochromic shifts of both the Soret (422-426 nm) and the Q-band a (550-559 nm) together with an increase of the intensity of both Q-bands (α and β) (Figure S26).[40] We therefore assume that such modifications of the absorption features result in improved photosensitization efficiency. The observed increase in fluorescence quantum yield (by a factor 1.6) when **4,4'-bipy** is bound within **1** confirmed this assumption (Figure S27).

The bathochromic shift and higher band intensity in **4,4'-bipy⊂1** compared to **1** is confirmed by the TD-CAM-B3LYP data. Figure 7 shows the sensitization mechanism and the energy levels involved. The calculated bathochromic shift for the absorbance, fluorescence and triplet energies upon encapsulation of **4,4'-bipy** is 0.1 - 0.15 eV (Table 1). This is in agreement with the experimental trend, although the experimental shift of approximately 0.02 eV in absorbance and fluorescence is somewhat overestimated. The ability to generate $^1O_2$ will be favoured, among other factors, by a porphyrin triplet energy that should be higher, but as close as possible, to the singlet triplet energy gap of oxygen, which is 0.98 eV (1269 nm), Following this argumentation, the lower triplet energy calculated for **4,4'-bipy⊂1** (T_1 = 1.50 eV) compared to **1** (T_1 = 1.65 eV) implies a higher probability of oxygen sensitization, which is consistent with the experimental data. In addition, the calculated oscillator strength for the lowest excited states of **4,4'-bipy⊂1** is approximately twice as high as that of the empty capsule (see ESI for details), which is also consistent with the stronger absorption of **4,4'-bipy⊂1** observed in the spectra.

Table 1. Experimental[a] and computed (TD-CAM-B3LYP/SDD) photophysical data (S_1 absorption and fluorescence bands, and adiabatic S_1 and T_1 energies) of prism **1** and the **4,4'-bipy⊂1** complex.

		Experimental		TD-CAM-B3LYP/SDD
		λ□[nm]	E_{rel} [eV]	E_{rel} [eV]
1	Absorption[b]	552, 592	2.24, 2.09	2.32
	Fluorescence[b]	601, 652	2.06, 1.90	2.27
	S_1 adiabatic[c]			2.30
	T_1 adiabatic[d]			1.65
4,4'-bipy⊂1	Absorption[b]	560, 597	2.21, 2.08	2.23
	Fluorescence[b]	606, 659	2.04, 1.88	2.18
	S_1 adiabatic[c]			2.21
	T_1 adiabatic[d]			1.50

[a] Concentration $1 \cdot 10^{-6}$ mol·l^{-1}; fluorescence spectra obtained with excitation at 560 nm. [b] Experimental data in CH_2Cl_2. [c] Difference between S_1 and S_0 energies at their corresponding geometries. [d] Difference between T_1 and S_0 energies at their corresponding geometries.

Using the **ZnTPP** photosensitizer in combination with **4,4'-bipy** (Figuree 4 and S24) or **(*m*-Py)exTTF** (Figure S25) did not affect the rates of $^1O_2$ generation in comparison with **ZnTPP** alone (Figure 6). This result can be correlated with the lack of modification of the UV-vis absorption spectra of **ZnTPP** in the presence of **4,4'-bipy** (Figure S26). These observations highlight the crucial role of the cage nature of **1** that allows for a strong axial ligation of pyridine-based ligands simultaneously to both Zn-porphyrins moieties,[20] even in highly diluted conditions (1.3 x 10^{-6} M).[41]

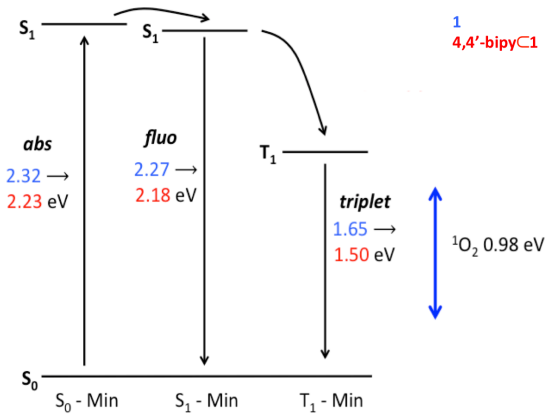

Figure 7. Energy levels involved in the singlet oxygen sensitization mechanism by **1** and **4,4'-bipy⊂1** (blue and red figures, respectively).

pH-dependent $^1O_2$ production: the Cu^{II}-based prism 2.

The use of a metal-organic capsule as photosensitizer raises the question of the influence of metallic centers over the photochemistry of the suprastructure. Indeed, a recent study on a BODIPY-based metal-organic capsule ($Fe^{II}_4L_6$) photosensitizer showed a modest quantum yield of singlet oxygen generation compared to well-established BODIPY photosensitizers. It was proposed that Fe^{II} metal centers could be responsible for the lowering of the quantum yield of $^1O_2$ generation by reducing the spin-orbit coupling necessary for efficient intersystem crossing.[42] Furthermore, several transition-metal complexes (Ni^{II}, Cu^{II}, Ag^{II}) are reported in the literature as moderate to excellent excited-state quenchers.[43] In particular, the paramagnetic Cu^{II}, with its d^9 valence electron configuration, is paramagnetic, which has been shown to increase the quenching efficiency. The Zn-porphyrin (ZnP) fluorescence quenching upon binding of Cu^{2+} ions to the periphery of the porphyrin has been reported through the synthesis of porphyrin-metal receptor dyads. [44] Steady-state fluorescence and lifetime measurements have demonstrated that the photo-excited singlet state of ZnP, ^{1}(ZnP)*, is quenched by a pendant [Cu^{II}(edta)] complex tethered to the ZnTPP chromophore through intramolecular photo-induced ET reaction.[45] Furthermore, the significant quenching of the emission and photosensitizing properties of the **Zn-TCPP** moieties of a metal–organic framework nanoparticle, have been very recently achieved by using Cu^{2+} ions as metal nodes of the network.[46]

To investigate the effect of the bridging metal ion in our self-assembled Zn-porphyrin prismatic capsules, the photosensitizing properties of Cu^{II}-based prism **2**, the copper-analogue of **1** (Figure 8), were tested.[47] As expected, the time-dependent plot of DPA absorbance in the presence of the soluble **2** (1.3 mol%) displayed a negligible decay rate, similar to the one observed in the absence of photosensitizer (Figure S28). Furthermore no degradation of **(m-Py)exTTF** was observed upon its exposition to light and air in the presence of **2** (4.0 mol%, 3 h, Figure S29), confirming the lack of $^1O_2$ production.

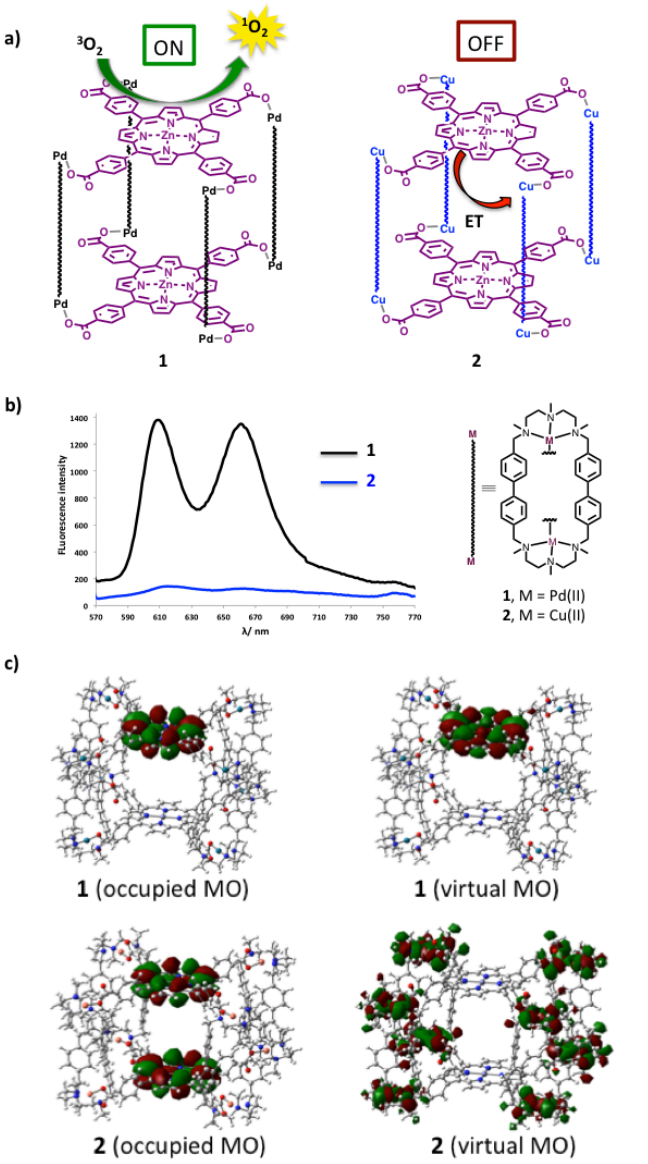

Figure 8. a) Schematic illustration of the "ON" and "OFF" states of the photosensitized production of $^1O_2$ respectively found in **1** and **2** (**ET**: Electron Transfer). b) Superimposed fluorescence emission spectrums of **1** and **2** in CH_3CN under Argon atmosphere (1 x 10^{-6} M, excitation at 560 nm). c) Representative orbitals involved in the lowest excited states of **1** and **2**.

The quenching of the excited states of the Zn-porphyrin moieties by the Cu(II)-macrocycle, was further confirmed by studying the fluorescence emission of **2**, which revealed a severe quenching resulting in a very low quantum yield value in CH_3CN (Φ_F = 0.00075) (Figure 8, S30). Finally, it should be noted that the quenching of the $^1O_2$ production observed for **2** is not affected by the encapsulation of **4,4'-bipy** (Figure S28).

The quenching mechanism in the Cu(II)-based capsule **2** is due to the existence of a manifold of low-lying excited states below the porphyrin Q-bands which are associated to the d^9

configuration of the Cu(II) atoms. According to TD-CAM-B3LYP calculations, the lowest excited states of **2** are a group of CT states from the porphyrin A_{1u}- and A_{2u}-like orbitals to the empty *d* orbitals of the Cu atoms (see representative orbitals in Figure 8c) at 0.25 - 0.27 eV, followed by a group of d-d metal centred states at 0.33 eV, and a group of ligand(biphenyl)-to-metal(Cu) charge transfer states of the side ligands between 1.35 and 1.39 eV (see Table S5). There are further groups of states around 2 eV. This suggests that the quenching of the porphyrin states in **2** occurs through decay to the low-lying states involving the Cu(II) atoms ultimately leading to electron transfer. Triplet sensitization is no more possible, energetically, from these states.

A common strategy to obtain activatable photosensitizers (a-PS) consists of maintaining the photosensitizer in a quenched state prior to a molecular activation that turns ON the photosensitizer. Quenching through Förster resonance energy transfer (FRET), induced electron transfer, and self-quenching are particularly useful strategies for efficient a-PS design.[48] The Zn-porphyrin moieties of **2** are in a quenched state (OFF-state) that deactivates $^1O_2$ generation and fluorescence. Contrary to a rigid covalent assembly, the "tunable" nature of metal-coordination bonds in **2** might allow for a reversible liberation of the porphyrin units. The latter would no longer held in close proximity to the metal centers and should therefore produce $^1O_2$ (ON-state). The reversible disassembly/reassembly of cage **2** was monitored by ^{1}H-NMR (Figure S31), ESI-HRMS (Figure S32) and UV-vis (Figure S33) upon addition of triflic acid and Et_3N respectively. To confirm ON/OFF switching of the photosensitization capability, **(*m*-Py)exTTF** was exposed to natural light and air in a $CH_3CN/DMF/CH_2Cl_2$ 1:2:20 solvent mixture for one hour in the presence of **2** (4.0 mol%) and Et_3N (8 equiv.) or CF_3SO_3H (8 equiv.). In the presence of Et_3N, no photo-oxidation of **(*m*-Py)exTTF** could be detected. Interestingly, in the presence of triflic acid, **(*m*-Py)exTTF** was fully converted into **P2**, **P3** and **AQ** oxidation products, accounting for a $^1O_2$ production (Figure S34). We thus monitored the ability of **2** to reversibly generate $^1O_2$ upon its disassembly/reassembly, by tracking the rate of the reaction of $^1O_2$ with DPA (Figure 9). A solution containing both DPA (8.27×10^{-3} M) and **2** (1.1 mol%) in a DMF/CH_2Cl_2 (1:2.5) solvent mixture, was irradiated at 575nm under air upon subsequent additions of Et_3N and CF_3SO_3H. The DPA absorption intensity was followed by UV-vis measurements (Figure S35). Interestingly, the DPA consumption clearly reveals that the $^1O_2$ production can be controlled through the addition of acid and base (Figure 9).

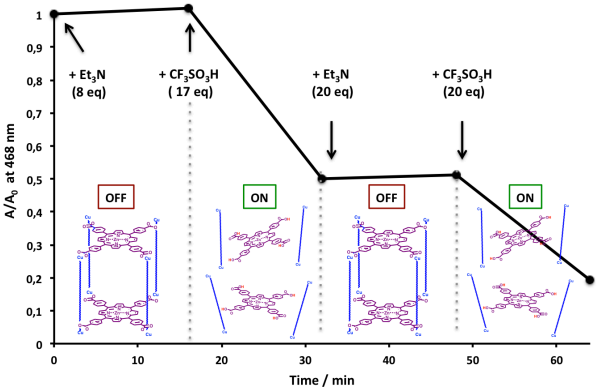

Figure 9. Time dependent decay rate of DPA (8.27×10^{-3} M in CH_2Cl_2/DMF (1:2.5)), in the presence of **2** (1.1 mol%), upon sequential additions of Et_3N and CF_3SO_3H, irradiation at 575 nm under air atmosphere.

Control experiments using the monomeric photosensitizer **Zn-TCPP** in combination with the copper(II) salt $Cu^{II}(OTf)_2$ were conduced under identical experimental conditions. Addition of $Cu^{II}(OTf)_2$ (4 equiv.) to a solution of **Zn-TCPP** in its carboxylate form (deprotonated by Et_3N, 4 equivalents) in a DMF/CH_2Cl_2 (1:2.5) solvent mixture, instantly led to the precipitation of the porphyrin which might result from the formation of insoluble oligomers $[(\textbf{Zn-TCPP})\text{-}Cu^{II}]_n$. Furthermore, the addition of 4 equiv. of CF_3SO_3H to the latter mixture did not recover the soluble **Zn-TCPP**. Interestingly, addition of $Cu^{II}(OTf)_2$ (4 equiv.) to a solution of the carboxylic-acid form of **Zn-TCPP** did not quench the $^1O_2$ production upon mixing but the favoured Cu-carboxylate complexation occurred after 10 minutes affording the same precipitate and totally quenching the $^1O_2$ production (Figure S36). The behavior of **2** is markedly different as both the cage **2** and the protonated **Zn-TCPP** and macrocyclic dicopper(II) complex arising from its reversible disassembly, were fully soluble, illustrating the benefits of the well-defined supra-structure of **2**, which prevent the formation of insoluble oligomeric species. Futhermore, it should be noted that identical control experiments (**Zn-TCPP** in combination with 4 equivalents of $Cu^{II}(OTf)_2$) were conducted in the presence of 4 equivalents of the nitrogenated chelating ligand *N,N,N',N',N"*-pentamethyldiethylenetriamine. Addition of this ligand prevents the formation of the insoluble oligomers and quench the $^1O_2$ production (Figure S36). However, in this case, the $^1O_2$ production is not turned-on upon addition of 4 equivalents of CF_3CO_3H and the addition of 8 equivalents of acid only lead to a very weak photooxidation of the DPA (15% convertion after 26 min). Clearly, this system (which mimics the structure of cage **2** but in a monomeric way) fails at reproducing the fine-tuning of $^1O_2$ production as observed for **2**.

Finally, since both cages **1** and **2** are reported as efficient receptors of fullerene derivatives with remarkably strong binding constants for C_{70},[47,49] we posed ourselves the question of what would be the effect of combining the dormant photosensitizer **2** with another $^1O_2$ photosensitizer such as C_{70}.[50] Cage **2**, which does not produce $^1O_2$, was used as a host to study the $^1O_2$ photosensitization ability of the encapsulated C_{70} in $\textbf{C}_{70}\subset\textbf{2}$. Interestingly, the use of catalytic amount of $\textbf{C}_{70}\subset\textbf{2}$ (1.3 mol%) in

CH_3CN/CH_2Cl_2 (9:1) leads to a DPA decay similar to the one observed for **1** (Figure 10, S37). C_{70} can therefore produce $^1O_2$ even when encapsulated inside the porphyrin-based nanocapsule. The use of C_{70} as photosensitizer is usually limited by its lack of solubility in common organic solvent. Inclusion of fullerene inside self-assembled mettalosupramolecular receptors is known as an efficient strategy in order to increase their solubility.[51] The particularly high affinity of **2** toward C_{70} ($K_a \approx 1.8\ 10^7\ M^{-1}$)[47] allows for solubilisation and transport of C_{70} photosensitizer into organic solvent such as CH_3CN or CH_2Cl_2, even in highly diluted conditions (1.3×10^{-6} M). The ability of **C_{70}⊂2** to generate $^1O_2$ in different solvent mixtures has been monitored by DPA trapping. The oxygen generation efficiency of **C_{70}⊂2** and C_{70} in toluene/CH_3CN (9:1) are modest with respectively 4% and 7 % conversion after 35 min of irradiation. According to the literature, the lifetime of singlet oxygen shows a strong solvent dependence. The reported $^1O_2$ lifetime in toluene, CH_3CN and CH_2Cl_2 at room temperature, are respectively 29, 75 and 91 µs.[52] Interestingly, when CH_2Cl_2 replaced toluene, a much higher $^1O_2$ generation efficiency of **C_{70}⊂2** was observed with 26% conversion of DPA (Figure 10, S38). C_{70} alone is not soluble in the later solvent mixture.

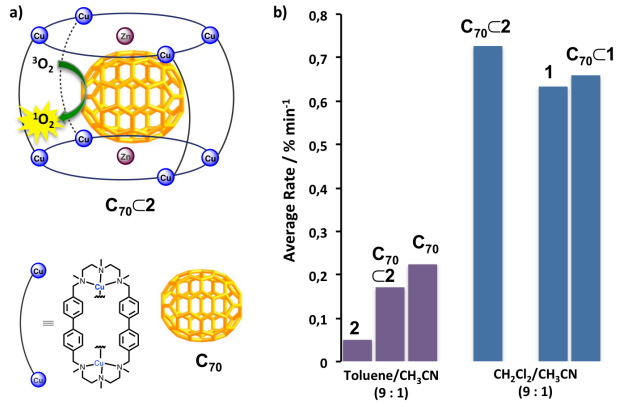

Figure 10. (a) Schematic representation of the **C_{70}⊂2** host-guest photosensitizer. (b) Average decay rate of DPA (0.1×10^{-3} M) within a 45 min irradiation time, using **1**, **C_{70}⊂1** , **2**, **C_{70}⊂2**, or **C_{70}** as photosensitizers (1.3 mol%) in toluene/CH_3CN (9:1) (purple) or CH_2Cl_2/CH_3CN (9:1) (blue).

This strong solvent effect can therefore be explained by the longer lifetime of $^1O_2$ in CH_2Cl_2 compared to toluene.[53] Aiming at avoiding the solvent quenching effect of toluene, the Zn-porphyrin-based nanocapsule **2** can therefore be used as a soluble cargo for the C_{70} photosensitizers without quenching its $^1O_2$ production efficiency. Finally, it should be noted that similar $^1O_2$ generation rates were observed for the empty capsule **1** or the **C_{70}⊂1** host-guests adduct (Figure S39).[54]

Conclusion

We have shown that the self-assembled cofacial Zn-porphyrin prisms **1** and **2** can be respectively used as robust $^1O_2$ photosensitizers and activatable photosensitizer. Indeed, the bridging metals Pd^{II} and Cu^{II} found in **1** and **2**, respectively, led to the formation of markedly different supramolecular photosensitizers with distinct photosensitizing properties. The production of $^1O_2$ was studied through the oxygenation of two anthracene-based substrates, the $^1O_2$ quencher DPA and the extended-TTF guest **(*m*-py)exTTF**.

The Pd^{II}-based supra-structure of **1** appears as a good compromise between efficiency and stability towards photobleaching. **1** displays a very similar photosensitizing efficiency comparing to the **ZnTPP** reference but with remarkably enhanced photostability, thus being a particularly robust catalyst for singlet oxygen production. The improved $^1O_2$ resistance observed for **1** compared to **ZnTPP** can be explained owing to both the reduction of the electron density and increase of the sterical hindrance at the porphyrin centers. This self-assembly approach avoids tedious purification steps and synthesis redesign of the porphyrin subunit. It therefore provides an additional tool to prevent porphyrins self-decompositon.

On the other hand, the Cu^{II}-carboxylate coordination bonds involved in **2** allow for an adaptive system with switchable properties. In the prism, the photosensitization is switched off by electron transfer to the Cu^{II} atoms. We have demonstrated that **2** can be used as a dormant $^1O_2$ photosensitizer that can be turned ON/OFF upon the reversible disassembly of the supra-structure by protonation/deprotonation of the carboxylate moieties and liberation of the tetra-carboxyphenyl zinc porphyrin moieties in the carboxylic form (**Zn-TCPP**). Such switching behavior can not be reproduced using **Zn-TCPP** unit in combination with simple $Cu^{II}(OTf)_2$ due to the formation of insoluble structures, highlighting the crucial role of the supra-structure in **2**. Sensitizers that allow for reversible switching between ON and OFF states have attracted growing attention,[55] and pH-based approaches have the potential to induce tumor-selective damages due to the higher acidity of tumor tissue comparing to normal tissue.[56] This novel pH-dependent approach to exert control over the $^1O_2$ generation upon breaking a supramolecular cage might be of significant importance as it opens the door to systems merging $^1O_2$ production and drug delivery.

Contrariwise to conventional porphyrin-based photosensitizers, nanocages **1** and **2** allow for strong host-guest interactions that open new opportunities for a challenging guest-control over $^1O_2$ generation. When pyridine-based ligands are encapsulated through the axial binding of both Zn-porphyrin of **1**, the $^1O_2$ production is significantly enhanced by a factor 1.4 through a shift of the energy levels involved in the sensitization. Finally, despite cage **2** can not produce $^1O_2$ in its OFF form, C_{70} can be encapsulated and the photosensitization ability of C_{70} itself is not altered by its encapsulation in **2**, making it interesting cargo for transport and delivery of organic photosensitizers. Indeed, the association between fullerene and porphyrin is considered as a promising strategy toward the development of therapeutic weapons having both drug-delivery and imaging capabilities.[57]

Since self-assembled prims based on porphyrin subunit and metallo-macrocycle can be easily obtained, we envision that library of such supramolecular photosensitizers may be rapidly built. In particular, the use of alternative building blocks allowing

for water solubility will be of particular interest to further extend the research perspectives of porphyrin-based nanocages toward photodynamic therapy.

Acknowledgements

We thank Spanish MINECO (CTQ2015-70795-P, CTQ2016-77989-P, CTQ2015-69363-P), the Agence Nationale de la Recherche (ANR-14-CE08-0001 JCJC BOMBER to S.G.), and the Generalitat de Catalunya (2014 SGR 862, 2014SGR-1202 and posdoctoral grant to C.C.). X.R. and M.C. are also grateful for ICREA-Acadèmia awards. We thank STR UdG for technical support. Calculations were carried out at the Consorci de Serveis Universitaris de Catalunya.

Keywords: porphyrin-based metallocages • self-assembly • supramolecular photosensitizers • host-guest chemistry • singlet oxygen

[1] P.R. Ogilby, *Chem. Soc. Rev.* **2010**, 39, 3181.
[2] A. A. Ghogare and A. Greer*, Chem. Rev.* **2016**, 116, 9994−10034.
[3] N. A. Romero and D. A. Nicewicz*, Chem. Rev.* **2016**, 116, 10075–10166.
[4] M. Klaper and T. Linker*, J. Am. Chem. Soc.* **2015**, 137, 13744−13747.
[5] X.Ding and B.-H. Han, Angew. *Chem. Int. Ed.* **2015**, 54, 6536 – 6539.
[6] K.Liu, Y. Liu, Y. Yao, H. Yuan, S. Wang, Z. Wang, and X. Zhang, *Angew. Chem. Int. Ed.* **2013**, 52, 8285-8289.
[7] J. Hynek, J. Rathousky, J. Demel and K. Lang, *RSC Adv.* **2016**, 6, 44279 − 44287.
[8] J. Park, D. Feng, S. Yuan and H.C. Zhou, *Angew. Chem. Int. Ed.* **2015**, 54, 430 − 435.
[9] Y.Z. Chen, Z. U. Wang, J. Lu, S. H. Yu, H. L. Jiang, *J. Am. Chem. Soc.* **2017**, 139, 2035−2044.
[10] A. K. Bar, S. Mohapatra, E. Zangrando and P. S. Mukherjee, *Chem. Eur. J.* **2012**, 18, 9571 – 9579
[11] Y. Shi, I. Sanchez-Molina, C. Cao, T. R. Cook, and P. J. Stang, *J. Proc. Natl. Acad. Sci. U. S. A.* **2014**, 111, 9390
[12] N. Mihara, Y. Yamada, and K. Tanaka, *Bull. Chem. Soc. Jpn.* **2017**, 90, 427-435
[13] T. Nakamura, H. Ube, M. Shiro, and M. Shionoya, *Angew. Chem. Int. Ed.* **2013**, 52, 720 –723
[14] W. Brenner, T. K. Ronson, and J. R. Nitschke *J. Am. Chem. Soc.* **2017**, 139, 75−78
[15] N. Struch, C. Bannwarth, T. K. Ronson, Y. Lorenz, B. Mienert, N. Wagner, M. Engeser, E. Bill, R. Puttreddy, K. Rissanen, J. Beck, S. Grimme, J. R. Nitschke, and A. Lgtzen, *Angew. Chem. Int. Ed.* **2017**, 56, 4930 – 4935.
[16] F. J. Rizzuto and J. R. Nitschke, *Nat. chem.* **2017**, 9, 903 – 908.
[17] E. G. Percastegui, J. Mosquera, and J. R. Nitschke, *Angew. Chem. Int. Ed.* **2017**, 56, 9136 - 9140
[18] L. Schoepff, L. Kocher, S. Durot, and V. Heitz, *J. Org. Chem.* **2017**, 82, 5845−5851
[19] (a) S. H. A. M. Leenders, R. Gramage-Doria, B. and J. N. H. Reek, *Chem. Soc. Rev.* **2015**, 44, 433; (b) P. F. Kuijpers, M. Otte, M. Dürr, I.Ivanović-Burmazović, J. N. H. Reek, and B. de Bruin, *ACS Catal.* **2016**, 6, 3106−3112 ; (c) M. Otte, P. F. Kuijpers, O. Troeppner, I. Ivanovic´-Burmazovic´, J. N. H. Reek, and B. de Bruin, *Chem. Eur. J.* **2014**, 20, 4880 – 4884
[20] C. García-Simón, R. Gramage-Doria, S. Raoufmoghaddam, T. Parella, M. Costas, X. Ribas and J. N. H. Reek, *J. Am. Chem. Soc.* **2015**, *137*, 2680-2687.
[21] X. Wang, S. S. Nurttila, W. I. Dzik, R. Becker, J. Rodgers, and J. N. H. Reek, *Chem. Eur. J.* **2017**, 23, 14769 – 14777
[22] F. Schmitt, N. P.E. Barry, L. Juillerat-Jeanneret, B. Therrien, *Bioorg. Med. Chem. Lett.* **2012**, 22, 178–180
[23] F. Schmitt, P. Govindaswamy, O. Zava, G. Süss-Fink, L. Juillerat-Jeanneret and B. Therrien, *J Biol Inorg Chem.* **2009**, 14, 101–109
[24] C. Colomban, G. Szaloki, M. Allain, L. Gomez, S. Goeb, M. Sallé, M. Costas and X. Ribas, *Chem. Eur. J.* **2017**, 23, 3016 - 3022
[25] A. E. Jones, C. A. Christensen, D. F. Perepichka, A. S. Batsanov, A; Beeby, P. J. Low, M. R. Bryce, and A. W. Parker, *Chem. Eur. J.* **200**1, 7, 5, 973-978.
[26] J.-B. Giguere and J.-F. Morin, *J. Org. Chem.* **2015**, 80, 6767−6775.
[27] M. Yoshizawa, S. Miyagi, M. Kawano, K. Ishiguro, and M. Fujita, *J. Am. Chem. Soc.* **2014**, 126, 9172-9173.
[28] It should be noted that the same catalytic behaviour was observed when zinc−tetraphenylporphyrin (**ZnTPP**) was used as photosensitizer instead of **1** (Figure S13)
[29] a) S. Martins, J.P.S. Farinha, C. Baleizao and M.N. Berberan-Santos, *Chem.Commun.* **2014**, 50, 3317-3320. b) J. Hynek, J. Rathousky, J. Demel and K. Lang, *RSC Adv.*,**2016**, 6, 44279-44287.
[30] Irradiation of DPA (0,1 mM) in the presence of **(m-Py)exTTF** (6,5 mol%) afford the same observation indicating that **(m-Py)exTTF** itself is not able to generate singlet oxygen (Figure S14).
[31] L. Hou, X. Zhang, T. C. Pijper, W.R. Browne and B. L. Feringa, *J. Am. Chem. Soc.* **2014**, 136, 910−913.
[32] The lower activity per Zn-porphyrin center for **1** can be explained by the fact that, due to symmetry, the S_1 state at the ground-state minimum of **1** is distributed over the two porphyrin units, and upon relaxation, the excitation localizes on one of the porphyrin units (see Table S1 and related comment).
[33] S. J. Kim and E. T. Kool, *J. Am. Chem. Soc.* **2006**, 128, 6164-6171
[34] M. I. Burguete, F. Galindo, R. Gavara, S. V. Luis, M. Moreno, P. Thomasc and D. A. Russell, *Photochem. Photobiol. Sci.* **2009**, 8, 37–44
[35] J.A.S. Cavaleiro, H. Görner, P. S.S. Lacerda, J. G. MacDonald, G. Mark, M.G.P.M.S. Neves, R. S. Nohr, H. P. Schuchmannb, C. V. Sonntag and A. C. Toméa*, J. Photochem. Photobiol. A Chem.* **2001**, 144, 131–140.
[36] R. Bonnett and G. Martinez, *tetrahedron* **2001**, 57, 9513-9547.
[37] (a) T. Nakazono, A. R. Parent and K. Sakai, *Chem. Eur. J.* **2015**, 21, 6723-6726. (b) T. Nakazono and K. Sakai, *Dalton Trans.* **2016**, 45, 12649 – 12652.
[38] A. M. S. Silva, M.G. P.M. S. Neves, R. R. L. Martins, J. A. S. Cavaleiro, T. Boschi and P. Tagliatesta, *J. Porphyr. Phthalocyanines* **1998**, 2, 45–51.
[39] The conversion of $\mathbf{P_3}$ upon irradiation (575nm), in CH_2Cl_2/CH_3CN 9:1, under air, was followed by UV-vis. In the absence of photosensitizer only negligible decrease in the absorbance of $\mathbf{P_3}$ was observed (Figure S21). In the presence of **1** (4 mol%) or **ZnTPP** (4 mol%), the oxidative cleavage of $\mathbf{P_3}$ (0.042 mM) into $\mathbf{P_2}$ and **AQ** show a decay of the absorbance bands of $\mathbf{P_3}$ (at 355 and 458 nm) with clean isosbestic points (Figure S21). After 145 min of irradiation time, the experiments with **1** showed a $\mathbf{P_3}$ conversion of 83% when ZnTPP shows a lower conversion of 55% (Figure S22).
[40] H. L. Kee, J. Bhaumik, J.R. Diers, P. Mroz, M. R. Hamblin, D.F. Bocian, J. S. Lindsey, and D. Holten*, J Photochem Photobiol A Chem.* **2008**, 200, 346–355.
[41] The reported affinity constant of **1** toward pyridine-based ligands ($K_a > 10^6$ M^{-1}), is three orders of magnitude higher than that the one of monomeric analogues **ZnTPP** ($K_a \approx 10^3$ M^{-1}).[20]
[42] P. P. Neelakandan, A. Jiménez, J. D. Thoburn, and J. R. Nitschke, *Angew. Chem. Int. Ed.* **2015**, 54, 14378 –14382.

[43] J. R. McCarthy and R. Weissleder, *ChemMedChem* **2007**, 2, 360 – 365.

[44] (a) Y. Q. Weng, F. Yue, Y. R. Zhong, and B. Ye, *Inorg. Chem.* **2007**, 46, 7749-7755. (b) Y. Ding, W.-H. Zhu, and Y. Xie, *Chem. Rev.* **2017**, 117, 2203−2256.

[45] H. Takashima, H. Kawahara, M. Kitano, S. Shibata, H. Murakami and K. Tsukahara, *J. Phys. Chem. B* **2008**, 112, 15493–15502.

[46] Y. Ma, X. Li, A. Li, P. Yang, C. Zhang, and B. Tang, *Angew. Chem. Int. Ed.* **2017**, 56, 13752 – 13756

[47] C. Fuertes-Espinosa, C. García-Simón, E. Castro, M. Costas, L. Echegoyen, and X. Ribas, *Chem. Eur. J.* **2017**, 23, 3553 – 3557.

[48] J. F. Lovell, T. W. B. Liu, J. Chen, and G. Zheng, *Chem. Rev.* **2010**, 110, 2839-2857.

[49] C. García-Simón, M. Garcia-Borràs, L. Gómez, T. Parella, S. Osuna, J. Juanhuix, I. Imaz, D. Maspoch, M. Costas and X. Ribas, *Nat. Commun*. **2014**, *5*, 5557.

[50] R. Kumar, E. H. Gleibner, E. Gabrielle V. Tiu, and Y. Yamakoshi, *Org. Lett.* **2016**, 18, 184−187.

[51] C. García-Simón, M. Costas and X. Ribas, *Chem. Soc. Rev.*, **2016**, *45*, 40-62.

[52] (a) R. Schmidt, *J. Am. Chem. Soc.* **1989**, 111, 6983. (b) F. Wilkinson, W. P. Helman, A. B. Ross, *J. Phys. Chem. Ref. Data* **1995**, 24, 663. (c) A. A.Gorman, M. A. J. Rodgers, *Singlet Oxygen*; *Scaiano, J. C., Ed.; CRC Press: BocaRaton, Florida*, **1989**; Vol. II, pp 229.

[53] C. Schweitzer and R. Schmidt, *Chem. Rev.* **2003**, 103, 1685-1757.

[54] The similar $^1O_2$ generation rates observed for **1**, **C_{70}⊂1** and **C_{70}⊂2** suggest an inhibition of the photosensitization at the Zn-porphyrin centers of **1** upon fullerene encapsulation. The strong quenching of the fluorescence of the Zn-porphyrin units of **1** upon C_{70} encapsulation is indeed reported,[49] confirming this proposal. We therfore suggest that the putative inhibition of photosensitization at the porphyrin centers of **C_{70}⊂1** is balanced by the $^1O_2$ production by the C_{70} guest itself.

[55] H. Horiuchi, R. Kuribara, A. Hirabara, and T. Okutsu, *J. Phys. Chem. A.* **2016**, 120, 5554−5561.

[56] T. Torring, R. Toftegaard, J. Arnbjerg, P. R. Ogilby, and K.V. Gothelf, *Angew. Chem. Int. Ed.* **2010**, 49, 7923 –7925.

[57] C. Constantin, M. Neagu, R. M. Ion, M. Gherghiceanu and C. Stavaru, *Nanomedicine* 2, **2010**, 5 (2).

Entry for the Table of Contents (Please choose one layout)

Layout 2:

FULL PAPER

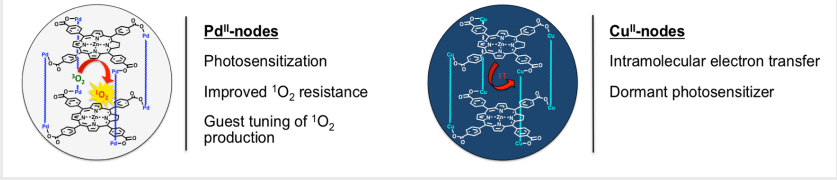

Text for Table of Contents

The benefits of using self-assembled cofacial Zn-porphyrins prisms as cage-like photosensitizers with tuneable photosensitizing properties are reported.

Cédric Colomban, Carles Fuertes-Espinosa, Sébastien Goeb, Marc Sallé, Miquel Costas, Lluis Blancafort and Xavi Ribas**

Page No. – Page No.

Self-assembled Cofacial Zinc Porphyrin Supramolecular Nanocapsules as tuneable $^1O_2$ Photosensitizers